Journal of Molecular Graphics and Modelling 28 (2009) 46–53

Contents lists available at ScienceDirect

Journal of Molecular Graphics and Modelling

journal homepage: www.elsevier.com/locate/JMGM

Ab initio molecular orbital calculations on specific interactions between urokinase-type plasminogen activator and its receptor

Keisuke Nagase [a], Hiroshi Kobayashi [b], Eri Yoshikawa [a], Noriyuki Kurita [a,*]

[a] Department of Knowledge-based Information Engineering, Toyohashi University of Technology, Tempaku-cho, Toyohashi, Aichi, 441-8580, Japan
[b] Department of Obstetrics and Gynecology, Nara Medical University, 840 Shijo-cho, Kashihara, Nara, 634-8521, Japan

ARTICLE INFO

Article history:
Received 21 January 2009
Received in revised form 27 March 2009
Accepted 1 April 2009
Available online 9 April 2009

Keywords:
Cancer metastasis
Cancer invasion
Urokinase-type plasminogen activator
uPAR
Molecular mechanics simulation
Fragment molecular orbital method
Molecular orbital calculation
Specific interaction
Protein–protein interaction

ABSTRACT

Cancer invasions and metastases are controlled by various proteases. In particular, the binding of urokinase-type plasminogen activator (uPA) to the uPA receptor (uPAR) existing on the surface of cancer cell is considered to be a trigger for cancer invasions. In the present study, we determined the structure of uPA and uPAR complex in water and investigated the specific interactions between uPA and uPAR by *ab initio* molecular orbital (MO) calculations based on fragment MO method. The result indicates that the 20–26 amino acid residues of uPA are important for the binding between uPA and uPAR, and that the electrostatic interactions between the charged amino acid residues existing in both uPA and uPAR have large contribution to the binding. The influence of crystal water molecules existing between uPA and uPAR was also investigated to be significant on the specific interactions between uPA and uPAR. These results are expected to be informative for developing new medicines blocking the binding of uPA and uPAR.

1. Introduction

By producing various proteases, cancer cells dissolve cell tissues such as extracellular matrix (ECM) and basement membrane to invade into blood vessel. The cancer cell passes through the blood vessel to the endothelial cells of other organs and invades them to develop a new metastases focus [1]. By repeating this process, cancer cells grow proliferously to put the cancer patient to death. It is thus expected that the inhibition of cancer invasion can suppress cancer metastasis, resulting in a good prognosis of the cancer patients.

Many types of medicines have been developed for suppressing cancer proliferation and metastases. They are usually administered to patients after the resection of primary tumor by surgical operation. In this case, physical strength of the patients is so weakened that they cannot take strong medicines with large side effect such as anti-cancer agents. Therefore, it is essential to develop a cancer metastasis suppressant with few side effects [2].

Recent biochemical experiment [3] elucidated that many types of proteases play essential roles in controlling the invasion mechanism of cancer cells. Among these proteases, urokinase-type plasminogen activator (uPA) is believed to play a key role in cancer invasion and metastasis [4,5]. uPA is a member of the serine protease family and is strongly implicated as a promoter of tumor progression in various human malignancies. The specific binding of uPA to the uPA receptor (uPAR) [6] existing on the surface of cancer cell is considered to be indispensable for promoting cancer invasion. The cancer cell assembles uPARs in its moving direction and binds uPA to uPAR. The uPA bound to uPAR efficiently converts the inactive plasminogen existing on the surface of cancer into the active serine protease plasmin, which directly or indirectly dissolves ECM components [7]. Therefore, it is expected that the blocking of the uPA and uPAR binding can inhibit cancer invasion and metastasis effectively.

In the previous structure analysis [8,9] for the complex of uPA and uPAR, it was elucidated that the amino-terminal fragment (ATF) of uPA, which is composed with the 1–132 amino acid residues of uPA, binds to uPAR. In particular, the 19–31 amino acid residues of ATF were found to be important for the binding of uPA to uPAR [10]. However, there is no experimental or theoretical study showing the complete three-dimensional structure of the uPA/uPAR complex.

In the present study, we determined stable structure of the uPA/uPAR complex in water by using classical molecular mechanics (MM) simulations. In addition, the specific interactions between uPA and uPAR were investigated at electronic level

* Corresponding author. Tel.: +81 532 44 6875; fax: +81 532 44 6875.
E-mail address: kurita@cochem2.tutkie.tut.ac.jp (N. Kurita).

1093-3263/$ – see front matter © 2009 Elsevier Inc. All rights reserved.
doi:10.1016/j.jmgm.2009.04.001

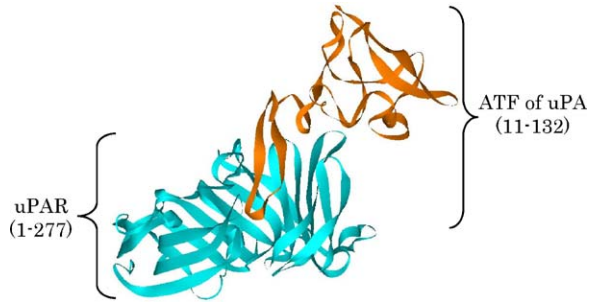

Fig. 1. Structure of the complex with ATF domain (orange) of uPA and uPAR (cyan) [10].

by using *ab initio* fragment molecular orbital (FMO) calculations. From these results, we elucidated which amino acid residues in both uPA and uPAR are important for the specific interactions between uPA and uPAR.

2. Details of molecular simulations

2.1. Optimization of uPA/uPAR structure in water

As a template structure of the uPA/uPAR complex, we employed the X-ray crystal structure registered in Protein Data Bank (PDB), whose PDB code is 2I9B [10]. This structure contains a tetramer of the complex with ATF of uPA and uPAR (Fig. 1) and 53 crystal water molecules. It is noted that the 162, 172, 200 and 233 amino acid residues of each uPAR are mutated from Asn to Gln, and that the positions of atoms for several amino acid residues of uPAR listed in Table 1 are missing in this PDB structure. It is thus necessary to mutate or supplement these amino acid residues of uPAR for obtaining the complete structure of the uPA/uPAR complex.

In the present study, we used the homology modeling program SWISS-MODEL [11] to construct the complete structure of uPAR monomer. In fact, the No.1 and No.2 monomers of uPAR in the PDB structure were used as the template structures for the modeling, because the other two monomers of uPAR have more deficiencies in amino acid residues, as shown in Table 1. Based on the No.1 and No.2 monomers, two complete structures of uPAR monomer were constructed.

In order to obtain the initial structures of the uPA/uPAR complex having crystal water molecules, we first extracted the No.1 and No.2 monomers of uPA/uPAR including crystal water molecules from the PDB structure [10]. Subsequently, the structure of uPAR in the uPA/uPAR complexes was replaced by the complete structure of uPAR monomer, so that two candidate structures of the complete uPA/uPAR complex containing crystal water molecules were obtained.

Finally, we optimized these two candidate structures by the classical MM method based on AMBER force field [12] with solvating water molecules considered explicitly. Indeed, we added hydrogen atoms to each candidate structure and optimized only their positions by the MM–MD calculation program AMBER9 [13]. In addition, we left crystal water molecules existing within a 8 Å distance from the uPA/uPAR structure and added solvating water molecules in a 8 Å shell around the structure. This solvated structure was optimized by AMBER9, in which the Parm99 [12] and TIP3 [14] force fields were used for uPA/uPAR and water molecules, respectively. The criterion for the convergence in structure optimization was set as the gradient norm is less than 0.01 kcal/(mol Å).

Table 1
Missing amino acid residues in each monomer of uPAR [10].

Monomer	1	2	3	4
Missing amino acid residues	106–109 132–136 246–249	106–109 132–136 246–249	32–34 83–93 106–109 132–136 246–249	32–34 83–93 106–109 132–136 246–249

2.2. Fragment MO calculations for the optimized uPA/uPAR complex

The solvated structures of uPA/uPAR have about 2700 water molecules, so that it is not practical to calculate their electronic properties by *ab initio* MO method. In the present study, we thus considered all crystal water molecules as well as some solvating water molecules existing within a 3 Å distance from the 17–41 amino acid residues of uPA and the 24–70, 122–171 amino acid residues of uPAR. These amino acid residues contribute to the specific interactions between uPA and uPAR [10]. The No.1 monomer of uPA/uPAR has 187 water molecules including 27 crystal water molecules, while the No.2 monomer has 176 water molecules including 23 crystal water molecules.

In order to investigate the binding energy between uPA and uPAR, the optimized solvated uPA/uPAR structure was divided into the following four structures. From their total energies obtained by FMO calculations, the binding energy between uPA and uPAR mediated by water molecules was estimated. Because it is not clear which monomer prefers to exist, we elucidated which monomer is more stable based on their obtained binding energies. It is noted that the basis-set superposition error was neglected in the analysis of binding energy between uPA and uPAR.

1. uPA/uPAR complex containing crystal and solvating water molecules (All).
2. uPA containing crystal and solvating water molecules (uPA + -water).
3. uPAR containing crystal and solvating water molecules (uPAR + water).
4. Crystal and solvating water molecules (water).

For the FMO [15–18] calculations, we used the ABINIT-MP program [19] developed by Nakano et al. The MP2 [20,21] method and the 6-31G basis-set were employed in FMO calculations, because the MP2/6-31G method was used in the previous FMO study [22] for protein–DNA complex to investigate the specific interactions between protein and DNA as well as the stacking interactions between DNA bases.

One of the advantages of FMO is that FMO can obtain the interaction energies between the fragments at only one SCF calculation with considering the effect of surrounding fragments. This pair interaction energy obtained by FMO is somewhat similar to the simple pair interaction energy computed by classical force field methods. However, in the FMO evaluation of the pair interaction energy, the influence from the other fragments is taken into account as a direct coulomb interaction. In the present study, the fragment size was set as one amino acid residue or one water molecule. We thus investigated the interaction energies between the amino acid residues of uPA and uPAR to elucidate which amino acid residues are important for the binding between uPA and uPAR. In addition, the effect of water molecules on the specific interactions between uPA and uPAR was investigated.

3. Results and discussion

3.1. Structure of uPA/uPAR complex in water

In order to confirm the adequacy of the monomer structures of uPA/uPAR obtained by SWISS-MODEL [11], we first compared

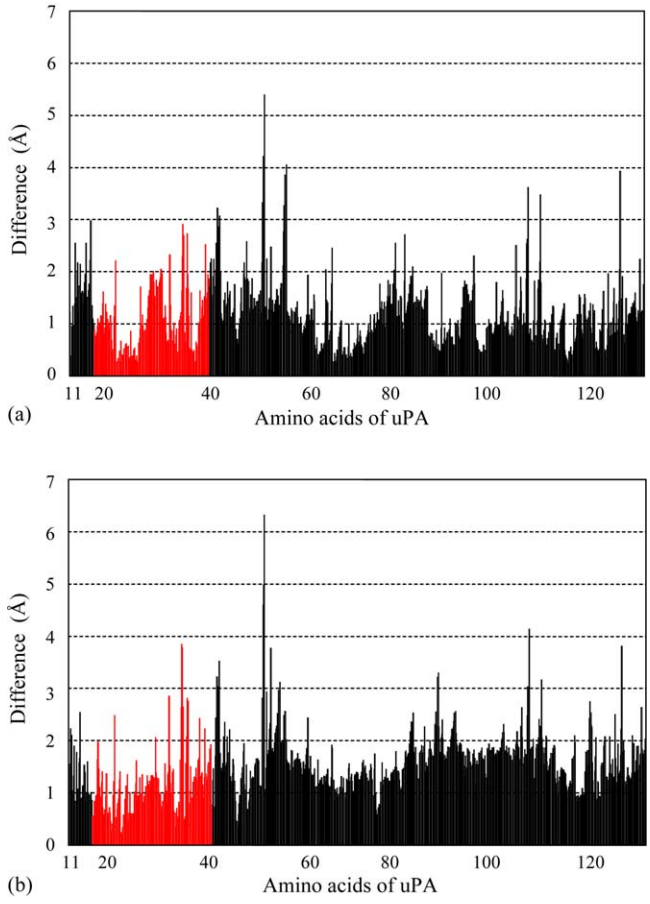

Fig. 2. Sum of deviations for each atom including hydrogen atoms of a given amino acid residue of uPA between the optimized and experimental [10] structures; (a) No.1 monomer and (b) No.2 monomer. The residues 17–41 of uPA contributing to the specific interaction between uPA and uPAR are shown in red.

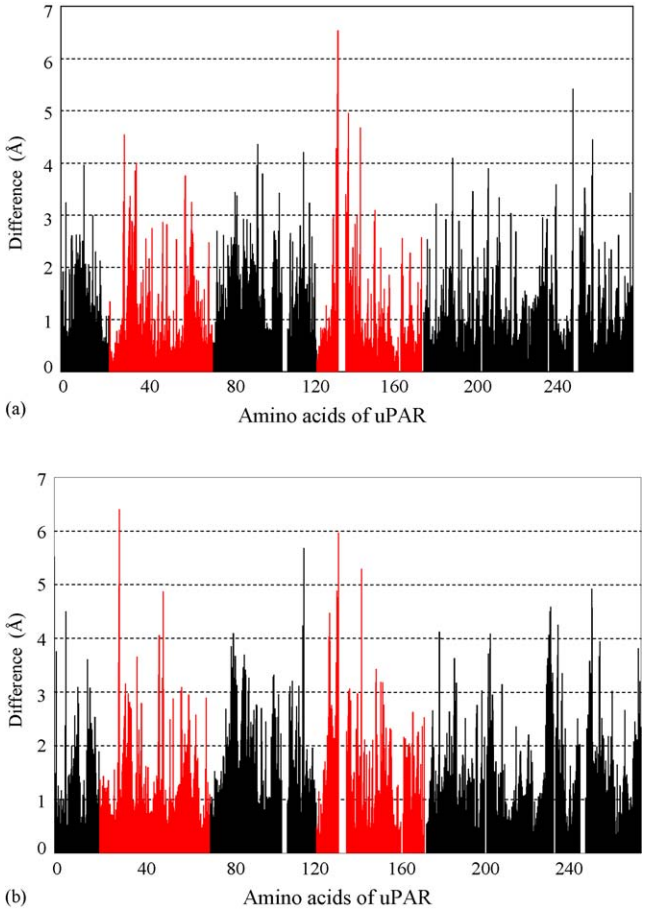

Fig. 3. Sum of deviations for each atom including hydrogen atoms of a given amino acid residue of uPAR between the optimized and experimental [10] structures; (a) No.1 monomer and (b) No.2 monomer. The residues 24–70 and 122–171 of uPAR contributing to the specific interaction between uPA and uPAR are shown in red.

them with the experimental one [10]. The RMSD (Root Mean Square Deviation) values between the obtained and the experimental structures for all heavy atoms of the amino acid residues except for the missing or mutated parts are 0.30 Å for both the No.1 and No.2 monomers. Therefore, it is confirmed that these obtained structures by SWISS-MODEL are comparable to the experimental one. We then optimized these structures by the classical MM method based on AMBER force field [12] with solvating water molecules considered explicitly. The RMSD values between the optimized and the experimental structures are 1.33 and 1.58 Å for the No.1 and No.2 monomers, respectively. These deviations are not negligible. In order to check which parts of uPA or uPAR have large deviation, we investigated the sum of deviations for each atom including hydrogen atoms of a given residue of uPA and uPAR. Figs. 2 and 3 show the results for the uPA and uPAR parts, respectively.

The 17–41 amino acid residues of uPA were considered important for the specific interactions between uPA and uPAR in the experiment [10]. As shown in Fig. 2a, among these amino acid residues, the 29, 30, 35 and 36 residues of the No.1 monomer have large deviation, while the deviations for the 23–26 residues are small. As for the No.2 monomer, Fig. 2b indicates that the 35 and 36 amino acid residues have large deviation, and that the structural deviation for the 23–26 residues is larger than that in the No.1 monomer shown in Fig. 2a.

The structural differences between the optimized and the experimental structures for each amino acid residue in uPAR are shown in Fig. 3a and b. It is noted that the 162, 172, 200 and 233 amino acid residues of uPAR are mutated from Asn to Gln, so that the structures of these amino acid residues are not compared. The 24–70 and 122–171 amino acid residues of uPAR are considered to contribute to the specific interactions between uPA and uPAR. As shown in Fig. 3a, among these amino acid residues, the 30, 131, 137 and 142 residues have large deviation in the No.1 monomer. In contrast, for the No.2 monomer, the 30, 47, 49, 128, 131 and 142 residues have large deviation as shown in Fig. 3b.

We considered that these deviations of uPA and uPAR structures from the experimental ones may come from the error of AMBER force field in structure optimizations or/and the effect of solvation around the uPA/uPAR complex. In principle, the structure

Table 2
Total energies (T.E.) (kcal/mol) for each component of the optimized structures of solvated uPA + uPAR complex and estimated binding energies (B.E.) (kcal/mol) between uPA and uPAR. B.E. = T.E. (uPA + uPAR + water) − T.E. (uPA + water) − T.E. (uPAR + water) + T.E. (water).

Monomer	All	uPA + water	uPAR + water	Water	B.E.
1	−114360910.58	−41395559.40	−81895890.19	−8931724.29	−1185.29
2	−113835371.91	−40153555.93	−81370227.62	−8406197.90	−1187.08

Table 3
Interaction energies (I.E.) (kcal/mol) between Lys23 of uPA and some amino acid residues of uPAR.

Amino acid residues of uPAR	I.E.
Asp140	−93.97
Thr127	−61.87
Asp254	−38.61
Glu183	−32.36
Phe256	−27.69
Asp124	−27.63
Asp141	−25.53
Asp163	−23.38
Glu185	−22.40
Glu132	−20.94

Table 4
Interaction energies (I.E.) (kcal/mol) between the amino acid residues around Lys23 of uPA and uPAR.

Amino acid residues of uPA	I.E.
Val20	−22.92
Ser21	−27.00
Asn22	−40.94
Tyr24	−33.43
Phe25	−61.18
Ser26	−36.74

optimization by using *ab initio* MO method is possible. However, it is not practical to optimize the solvated uPA/uPAR complex by the *ab initio* method. Therefore, in the present study, we adopted the structure optimized by the classical MM method based on AMBER force field. In addition, because the purpose of the present study is to investigate the specific interactions between uPA and uPAR existing on the surface of cancer cell, we employed the optimized structure for the solvated uPA/uPAR monomer.

3.2. Specific interactions between uPA and uPAR

For the optimized structures of the solvated uPA/uPAR monomers, the binding energy between uPA and uPAR was investigated by FMO method with the crystal and solvating water molecules considered explicitly. Table 2 lists the total energies for the each part of the solvated uPA/uPAR and the binding energies between uPA and uPAR estimated by the equation shown in Table 2. The obtained binding energies are considerably large for the both monomers, indicating that uPA binds strongly to uPAR. It is noted that we investigated the interaction energies in vacuum with crystal and solvating water molecules considered explicitly. This may cause the large binding energy between uPA and uPAR. We investigated the specific interactions between the amino acid residues of both uPA and uPAR for the structure of the No.2 monomer, because the binding energy for the No.2 monomer is larger than that for the No.1 monomer.

In order to elucidate which amino acid residues of uPA are important for the binding to uPAR, we investigated the interaction energies between each amino acid residue of uPA and uPAR by FMO method. Fig. 4 shows the total interaction energies between each amino acid residue of uPA and all amino acid residues of uPAR. The positively charged amino acid residues Lys23, Lys46, Lys61 and Lys98 were found to have large attractive interaction with uPAR. In contrast, the negatively charged Glu43, Asp45 and Asp12 have repulsive interaction with uPAR.

As shown in Fig. 4, the Lys23 of uPA binds most strongly to uPAR. To elucidate the reason of this large interaction, we investigated the interaction energies between Lys23 and each amino acid residue of uPAR in detail. Table 3 lists the amino acid

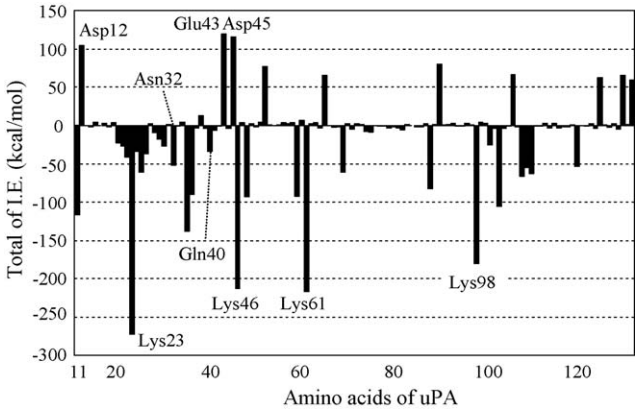

Fig. 4. Total of interaction energies (I.E.) between each amino acid residue of uPA and uPAR.

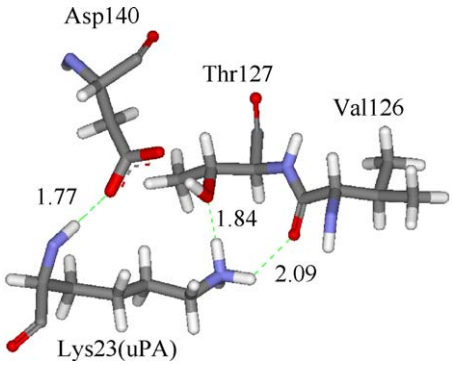

Fig. 5. Hydrogen bonding interactions (Å) between Lys23 of uPA and some amino acid residues of uPAR. Small red atoms are oxygen atoms of carbonyl groups.

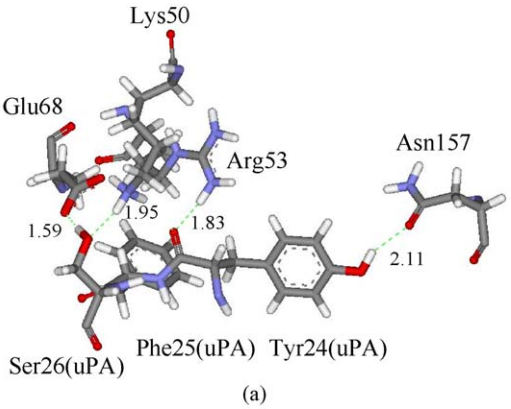

Fig. 6. Hydrogen bonding interactions (Å) between amino acid residues of uPA and those of uPAR; (a) Tyr24, Phe25 and Ser26 of uPA and uPAR, (b) Cys19, Val20, Ser21 and Asn22 of uPA and uPAR. Small red atoms are oxygen atoms of carbonyl groups.

Table 5
Distances (Å) of hydrogen bonds and interaction energies (I.E.) (kcal/mol) between the amino acid residues around Lys23 of uPA and those of uPAR.

Amino acid residues of uPA	Amino acid residues of uPAR	Distance	I.E.
Val20	Lys139	2.13	−19.86
Ser21	Asp140	2.00	−14.25
Asn22	Asp140	1.89	−21.49
Tyr24	Asn157	2.11	−9.64
Phe25	Arg53	1.83	−37.27
Ser26	Lys50	1.95	−18.70
Ser26	Glu68	1.59	−14.94

residues of uPAR interacting strongly to Lys23 and its interaction energy in the decreasing order of interaction energy. The positively charged Lys23 interacts attractively with the negatively charged Asp and Glu amino acid residues of uPAR. In particular, as shown in Fig. 5, Lys23 is hydrogen bonded to the side chain of Asp140 of uPAR at 1.77 Å distance, so that the interaction energy between these amino acid residues is very large (−93.97 kcal/mol). In addition, the side chain of Lys23 is hydrogen bonded with Thr127 and the carbonyl oxygen atom of Val126 at 1.84 and 2.09 Å distances, resulting in the large (−61.87 kcal/mol) interaction energy between Lys23 and Thr127. The previous experiment [10] indicated that the amide hydrogen atom of Lys23 is hydrogen bonded to the oxygen atom of the side chain of Asp140, and that the NH_3 part of the Lys23 side chain is hydrogen bonded to the oxygen atom of the side chain of Thr127. The structure (Fig. 5) obtained by the present calculation is comparable to the experimental result. Therefore, it is concluded from Table 3 and Fig. 5 that the specific interactions between Lys23 of uPA and both Asp140 and Thr127 of uPAR are the most efficient for the binding between uPA and uPAR.

The amino acid residues around Lys23 of uPA also have large contribution to the binding between uPA and uPAR. Table 4 lists the interaction energies between these amino acid residues and uPAR. Among these amino acid residues, Phe25 and Asn22 have large attractive interaction energies to uPAR. In fact, as shown in Fig. 6a, Phe25 is hydrogen bonded to Arg53 of uPAR, while Asn22 is hydrogen bonded to Asp140 of uPAR (Fig. 6b). In order to elucidate which amino acid residues of uPAR are important for these interactions, we investigated the interaction energies and hydrogen bonding distances between the 20–26 amino acid residues of uPA and all amino acid residues of uPAR. As shown in Table 5, the 20–26 amino acid residues of uPA have at least one hydrogen bond with the amino acid residue of uPAR, indicating that the group of

Table 6
Total of interaction energies (I.E.) (kcal/mol) between the positively charged amino acid residues of uPA and all residues of uPAR.

Amino acid residues of uPA	Total of I.E.
Lys23	−272.66
Lys35	−138.13
Lys36	−90.19
Lys46	−212.60
Lys48	−92.66
Arg59	−92.26
Lys61	−216.79
Arg69	−61.20
Arg88	−82.29
Lys98	−179.89
Arg103	−105.14
Arg108	−66.17
Arg109	−55.28
Arg110	−62.65
Lys120	−53.67

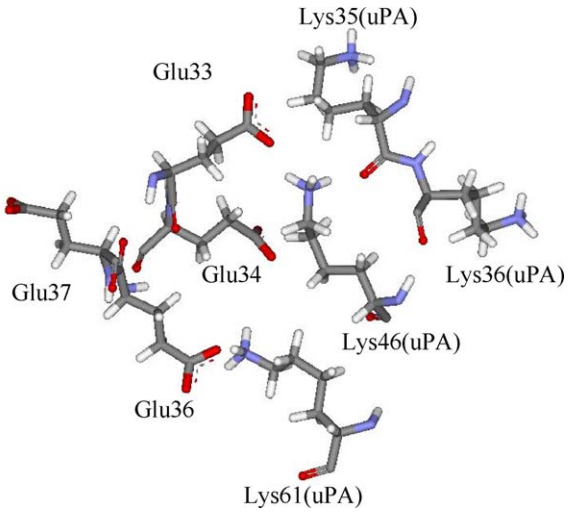

Fig. 7. Relative configurations for the positively charged Lys of uPA and the negatively charged Glu of uPAR. Small red atoms are oxygen atoms of carbonyl groups.

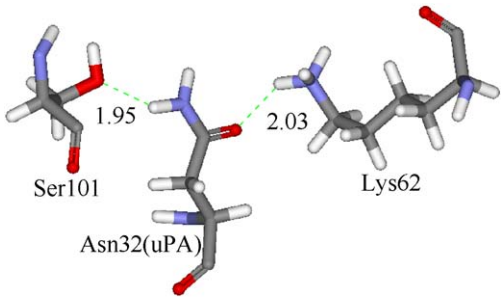

Fig. 8. Hydrogen bonding interactions (Å) between Asn32 of uPA and Lys62 and Ser101 of uPAR. Small red atoms are oxygen atoms of carbonyl groups.

these amino acid residues of uPA play an important role in the strong binding between uPA and uPAR. As shown in Table 3 and Fig. 5, Lys23 of uPA is strongly bound to Asp140 and Thr127 of uPAR. This strong binding is expected to move the 20–26 amino acid residues of uPA closer to uPAR, resulting in the large interaction energies between the 20–26 amino acid residues and uPAR shown in Table 5.

To clarify the contribution of the charged amino acid residues of uPA to the binding between uPA and uPAR, the interaction energies between the positively charged amino acid residues Lys and Arg of uPA and uPAR were investigated (Table 6). uPAR has 35 negatively charge amino acid residues (12 of Asp and 23 of Glu) and 28 positively charged amino acid residues (18 of Arg and 10 of Lys). It is thus expected that the positively charged amino acid residues of

Table 7
Attractive interaction energies (I.E.) (kcal/mol) between Cys11 of uPA and the amino acid residues of uPAR. The residues are listed in the decreasing order of the magnitude of their interaction energies.

Amino acid residues of uPAR	I.E.
Glu135	−32.46
Glu132	−32.34
Glu42	−28.35
Glu230	−21.07
Asp141	−20.36
Asp140	−19.51
Glu68	−18.37
Asp102	−18.13
Glu15	−17.00
Glu39	−16.88

Table 8
Repulsive interaction energies (I.E.) (kcal/mol) between Ala132 of uPA and the amino acid residues of uPAR. The residues are listed in the decreasing order of the magnitude of their interaction energies.

Amino acid residues of uPAR	I.E.
Glu34	14.29
Glu36	12.85
Glu33	11.48
Asp102	9.45
Glu37	8.78
Asp141	8.48
Glu39	8.35
Glu106	8.30
Asp11	7.70
Glu42	7.64

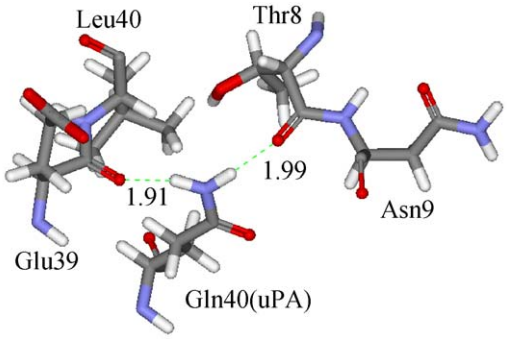

Fig. 9. Hydrogen bonding interactions (Å) between Gln40 of uPA and some amino acid residues of uPAR. Small red atoms are oxygen atoms of carbonyl groups.

uPA have attractive interaction with uPAR. As shown in Table 6, in particular, Lys23, Lys61, Lys46, Lys98, Lys35 and Arg103 of uPA have attractive interactions larger than 100 kcal/mol, so that these amino acid residues are important for the binding between uPA and uPAR. In addition, Lys61, Lys46, Lys35 and Lsy36 listed in Table 6 exist close to each other as shown in Fig. 7, and they interact with the negatively charged amino acid residues (Glu33, Glu34, Glu36 and Glu37) of uPAR. Therefore, it is elucidated that the group of the positively charged Lys of uPA have large attractive interaction with the group of the negatively charged Glu of uPAR,

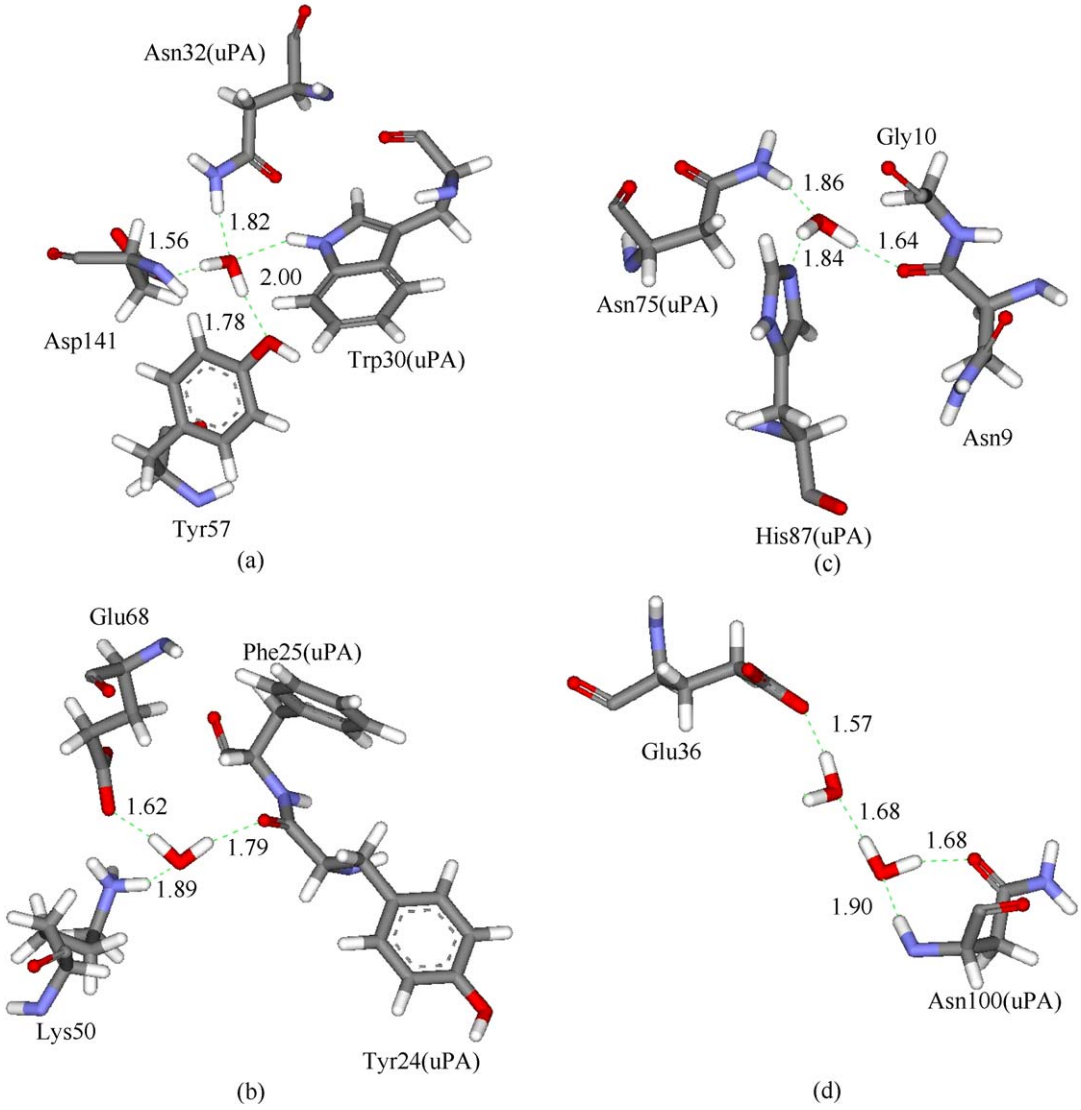

Fig. 10. Hydrogen bonding interactions (Å) between amino acid residues of uPA and uPAR bridged by crystal water molecules; (a) between Asn32 and Trp30 of uPA and Tyr57 and Asp141 of uPAR, (b) between Tyr24 and Phe25 of uPA and Lys50 and Glu68 of uPAR, (c) between Asn75 and His87 of uPA and Asn9 and Gly10 of uPAR, (d) between Asn100 of uPA and Glu36 of uPAR. Small red atoms are oxygen atoms of carbonyl groups.

and that these electrostatic interactions between these charged amino acid residues of uPA and uPAR are important for the binding between uPA and uPAR.

As shown in Fig. 4, Cys11 (N-terminal amino acid residue) and Ala132 (C-terminal amino acid residue) of uPA have large interaction energy with uPAR. These values are −115.88 and 59.79 kcal/mol, respectively. In the present calculation, the N- and C-terminal residues of uPA and uPAR are terminated by NH_3^+ and COO^-, respectively, so that Cys11 is positively charged and Ala132 is negatively charged. The interaction energies between Cys11 and the amino acid residues of uPAR are listed in Table 7, indicating that Cys11 has attractive interactions with the negatively charged amino acid residues Glu and Asp of uPAR. In contrast, Ala132 of uPA has repulsive interactions with the negatively charged amino acid residues Glu and Asp of uPAR, as shown in Table 8. These large interactions come from the charges of the NH_3^+ and COO^- terminations. Therefore, in the present study, we excluded Cys11 and Ala132 of uPA from the amino acid residues contributing to the specific interactions between uPA and uPAR.

As indicated in Fig. 3, the uncharged amino acid residues Asn32 and Gln40 of uPA have large interaction energies with uPAR. These values are −51.92 (Asn32) and −33.73 kcal/mol (Gln40), respectively. As shown in Fig. 8, Asn32 is hydrogen bonded to Lys62 and Ser101 of uPAR at the 2.03 and 1.95 Å distances. As a result, the interaction energies between Asn32 and Lys62, and Asn32 and Ser101 are −42.67 and −9.80 kcal/mol, respectively. Gln40 of uPA also interacts to Leu40 and Asn9 of uPAR as shown in Fig. 9. These hydrogen bond distances are 1.91 and 1.99 Å, respectively, resulting in the interaction energies −18.08 (between Gln40 and Leu40) and −10.24 kcal/mol (Gln40 and Asn9), respectively. These interactions between the uncharged amino acid residues of uPA and uPAR are weaker than those between the charged amino acid residues. However, it seems that they can contribute to determining the hydrogen bonded structure between uPA and uPAR.

3.3. Specific interactions between uPA and uPAR bridged by water molecules

In the present study, in order to model the state of the uPA/uPAR complex on the surface of cancer cell as accurate as possible, we considered crystal as well as solvating water molecules around the complex explicitly. From the FMO result for the solvated uPA/uPAR complex, the specific interactions between uPA and uPAR bridged by these water molecules are elucidated. As shown in Fig. 10, some amino acid residues of uPA make hydrogen bonds to the amino acid residues of uPAR via one or two crystal water molecules. In fact, five crystal water molecules bridge the interactions between uPA and uPAR, while there is no solvating water molecule bridging between uPA and uPAR.

The crystal water molecule shown in Fig. 10a bridges between Trp30/Asn32 of uPA and Tyr57/Asp141 of uPAR. The interaction energies between the water molecule and Trp30 and Asp32 are −5.20 and −8.58 kcal/mol, respectively. Moreover, the same water molecule is hydrogen bonded to the both Try57 and Asp141 of uPAR with the −7.63 and −22.00 kcal/mol, respectively. Therefore, it was elucidated that the crystal water molecule shown in Fig. 10a plays an important rule in making hydrogen bonds between these four amino acid residues.

In addition, we found that the crystal water molecule shown in Fig. 10b contributes to the hydrogen bonds between Phe25 of uPA and Lys50/Glu68 of uPAR. The interaction energies between the water molecule and Phe25, Lys50 and Glu68 are −15.41, −12.33 and −16.64 kcal/mol, respectively. In the same way, the crystal water molecule shown in Fig. 10c is hydrogen bonded to Asn75 and His87 of uPA as well as Gly10 of uPAR. Their interaction energies between the water molecule and the amino acid residues are −12.43 (Asn75), −16.69 (His87) and −17.75 kcal/mol (Gly10), indicating that the water molecule makes a large contribution to the binding between uPA and uPAR. As shown in Fig. 10c, the water molecule is hydrogen bonded to the carbonyl oxygen atom of the backbone between Gly10 and Asn9. In the present FMO calculation, this oxygen atom is grouped into the fragment of Gly10. As a result, the interaction energy between Gly10 and the water molecule becomes large.

Finally, we found that two crystal water molecules bridge Asn100 of uPA and Glu36 of uPAR, as shown in Fig. 10d. One of these water molecules is hydrogen bonded to Asn100 with −18.33 kcal/mol interaction energy, while the other water molecule is hydrogen bonded to Glu36 with −24.71 kcal/mol interaction energy. Moreover, these crystal water molecules are hydrogen bonded to each other with −8.86 kcal/mol. As the results, these crystal water molecules and the two amino acid residues construct the specific hydrogen bonding network shown in Fig. 10d. Therefore, the present FMO analysis considering crystal water molecules explicitly elucidates that the crystal water molecules shown in Fig. 10a–d have important contribution to the specific interactions between uPA and uPAR.

4. Conclusions

In the present study, we first optimized the solvated structure of uPA/uPAR complex by the classical molecular mechanics method (AMBER99) with water molecules considered explicitly. For the optimized structure, *ab initio* MP2/6-31G MO calculation based on the fragment MO method was performed to elucidate the following points on the specific interactions between uPA and uPAR.

(1) Positively charge amino acid residue Lys23 of uPA binds most strongly to uPAR by electrostatic interactions with Thr127 and Asp140 of uPAR.
(2) The 20–26 amino acid residues of uPA are hydrogen bonded to the amino acid residues of uPAR to strengthen the interaction between uPA and uPAR.
(3) Positively charged amino acid residues Lsy23, Lys61, Lys46 and Lys98 of uPA have large attractive interactions with the negatively charged uPAR.
(4) Five unique crystal water molecules shown in Fig. 10 have large contributions to the specific hydrogen bonding interactions between uPA and uPAR.

In the previous experiment [10], the 17–41 amino acid residues of uPA were considered to be important for the binding between uPA and uPAR. The present calculated results qualitatively agree with the experimental data. Therefore, based on the present results, we will propose some peptides composed with the amino acid residues strongly binding to uPAR as a new medicine blocking the binding of uPA to uPAR.

Acknowledgments

This work was supported in part by the grants from Iketani Science and Technology Foundation, Tatematsu Foundation, CASIO Science Promotion Foundation and Toukai Foundation for Technology.

References

[1] E. Ruoslahti, How cancer spreads, Sci. Am. 9 (1996) 48–55.
[2] H. Kobayashi, J. Gotoh, Y. Hirashima, M. Fujie, D. Sugino, T. Terao, Inhibitory effect of a conjugate between human urokinase and urinary trypsin inhibitor on tumor cell invasion in vitro, J. Biol. Chem. 270 (1995) 8361–8366.
[3] A.E. Baker, J.D. Leaper, The Plasminogen activator and matrix metalloproteinase systems in colorectal cancer: relationship to tumour pathology, Eur. J. Cancer 39 (2003) 981–988.

[4] M.M. Skelly, A. Troy, M.J. Duffy, H.E. Mulcahy, C. Duggan, T.G. Connell, D.P. O'Donoghue, K. Sheahan, Urokinase-type plasminogen activator in colorectal cancer: relationship with clinicopathological features and patient outcome, Clin. Cancer Res. 3 (1997) 1837–1840.
[5] L. Herszènyi, M. Plebani, P. Carraro, M. De Paoli, G. Roveroni, R. Cardin, Z. Tulassay, R. Naccarato, F. Farinati, The role of cysteine and serine proteases in colorectal carcinoma, Cancer 86 (1999) 1135–1142.
[6] R.W. Stephens, H.J. Nielsen, I.J. Christensen, O. Thorlacius-Ussing, S. Sorensen, K. Dano, N. Brunner, Plasma urokinase receptor levels in patients with colorectal cancer: relationship to prognosis, J. Natl. Cancer Inst. 91 (1999) 869–874.
[7] J. Romer, B.S. Nilsen, M. Ploug, The urokinase receptor as a potential target in cancer therapy, Curr. Pharm. Des. 10 (2004) 2359–2376.
[8] E. Appella, E.A. Robinson, S.J. Ullrich, M.P. Stoppelli, A. Corti, G. Cassani, F. Blasi, The receptor-binding sequence of urokinase. A biological function for the growth-factor module of proteases, J. Biol. Chem. 262 (1987) 4437–4440.
[9] K. Bdeir, A. Kuo, B.S. Sachais, A.H. Rux, Y. Bdeir, A. Mazar, A.A. Higazi, D.B. Cines, The kringle stabilizes urokinase binding to the urokinase receptor, Blood 102 (2003) 3600–3608.
[10] C. Barinka, G. Parry, J. Callahan, D.E. Shaw, A. Kuo, K. Bdeir, D.B. Cines, A. Mazar, J. Lubkowski, Structural basis of interaction between urokinase-type plasminogen activator and its receptor, J. Mol. Biol. 363 (2006) 482–495.
[11] T. Schwede, J. Kopp, N. Gues, M.C. Peitch, SWISS-MODEL: an automated protein homology-modeling server, Nucleic Acids Res. 31 (2003) 3381–3385.
[12] J. Wang, P. Cieplak, P.A. Kollman, How well does a restrained electrostatic potential (RESP) model perform in calculating conformational energies of organic and biological molecules? J. Comput. Chem. 21 (2000) 1049–1074.
[13] D.A. Case, T.E. Cheatham III, T. Darden, H. Gohlke, R. Luo, K.M. Merz Jr., A. Onufriev, C. Simmerling, B. Wang, R.J. Woods, The AMBER biomolecular simulation programs, J. Comput. Chem. 26 (2005) 1668–1688.
[14] W.L. Jorgensen, J. Chandrasekhar, J. Madura, M.L. Klein, Comparison of simple potential functions for simulating liquid water, J. Chem. Phys. 79 (1983) 926–935.
[15] K. Kitaura, T. Sawai, T. Asada, T. Nakano, M. Uebayashi, Pair interaction molecular orbital method: an approximate computational method for molecular interactions, Chem. Phys. Lett. 312 (1999) 319–324.
[16] K. Kitaura, E. Ikeo, T. Asada, T. Nakano, M. Uebayashi, Fragment molecular orbital method: an approximate computational method for large molecules, Chem. Phys. Lett. 313 (1999) 701–706.
[17] T. Nakano, T. Kaminuma, T. Sato, Y. Akiyama, M. Uebayashi, K. Kitaura, Fragment molecular orbital method: application to polypeptides, Chem. Phys. Lett. 318 (2000) 614–618.
[18] T. Nakano, T. Kaminuma, T. Sato, K. Fukuzawa, Y. Akiyama, M. Uebayashi, K. Kitaura, Fragment molecular orbital method: use of approximate electrostatic potential, Chem. Phys. Lett. 351 (2002) 475–480.
[19] T. Nakano, et al. http://www.ciss.iis.u-tokyo.ac.jp/rss21/.
[20] Y. Mochizuki, T. Nakano, S. Koikegami, S. Tanimori, Y. Abe, U. Nagashima, K. Kitaura, A parallelized integral-direct mp2 method with fragment molecular orbital scheme, Theor. Chem. Acc. 112 (2004) 442–452.
[21] Y. Mochizuki, S. Koikegami, T. Nakano, S. Amari, K. Kitaura, Large scale MP2 calculations with fragment molecular orbital scheme, Chem. Phys. Lett. 396 (2004) 473–479.
[22] K. Fukuzawa, Y. Komeiji, Y. Mochizuki, A. Kato, T. Nakano, S. Tanaka, Intra- and intermolecular interactions between cyclic-amp receptor protein and DNA: ab initio fragment molecular orbital study, J. Comput. Chem. 27 (2006) 948–960.